THE NEC2 RADIATION PATTERNS OF UNDER-SEGMENTED WIRE GRID MODELS OF A FIGHTER AIRCRAFT COMPARED TO MEASUREMENTS

O. Givati and APC. Fourie
University of the Witwatersrand, Johannesburg
Private Bag 3, P O WITS 2050, South Africa

ABSTRACT

This paper presents results of a NEC2 method of moments evaluation of VHF/UHF antennas on a wire grid model of a fighter aircraft. The study shows that practically useful radiation patterns results can be obtained when the grid model is considerably under-segmented in aircraft regions which are electrically far removed from the antennas. Normal modelling guide-lines requires approximately 35000 segments for the fighter grid model at 400 MHz; judicious under-segmentation gave useful results using a model comprising 5000 segments. This reduction in segments reduced computer time by a factor of 343 and memory requirements is reduced by a factor of 18. NEC2 radiation patterns are compared to measurements on a 1/10th scale model which was performed in an anechoic chamber compact range.

1 INTRODUCTION

The paper consider a study of radiation patterns from antennas mounted on a fighter aircraft. NEC2 [1] computed radiation patterns are used for subsequent statistical assessment of link performance for the aircraft during typical mission profiles. Wire grids and segments much longer than the recommended [1] 0.1λ were used in areas far removed from the antennas to reduce execution time and memory requirements. Measured results, as well as comparison to more densely segmented numerical models, were used to ensure that these violations of modelling rules still produced useful values. It may be argued that numerical modelling is superfluous when measured results are available, but this is not the case when considering that:

- measurements in only three principle planes were performed and compared to a subset of the computed values; the statistical link analysis requires full three dimensional pattern information which is difficult and time consuming to obtain by measurement.
- traditional engineering normally argues that measurements constitute the more definitive characterization of a system when compared with calculation. This is definitely not always the case with radiation pattern measurements, especially on scale models, and many electromagnetics engineers can attest to cases where more confidence can be placed on values obtained from calculation or simulation.

The engineer is hence in a difficult position. He has two methods giving two sets of results - both associated with some potentially large errors. On the positive side is the fact that the two sets of results were obtained using two entirely different methods, with appropriate techniques used in both cases to minimize errors. Qualitative agreement will definitely demonstrate the absence of major blunders in both methods, and engineering judgement and cost will dictate which set of results is likely to be more appropriate.

Valid numerical models, for the purpose of subsequent statistical link analysis, are hence those which show qualitative agreement with measured results. Quantitative comparison between the measured and computed radiation patterns is difficult and often misleading, because:

- errors may be large when comparing measured and computed values at specific angles, but such errors may only be due to a slight offset in the position of a radiation pattern null, for instance. Such small angular offsets are not of any concern when performing statistical analysis of communication link performance.
- the existence of significant measurement errors also frustrate efforts to call the deviation from measured values "simulation errors".

It is hence evident that some of the more traditional quantitative measures of agreement between measured and computed results will be less useful and often meaningless. It is indeed left to the reader to assess the presented comparisons between measured and computed results and decide on their worth for a specific application. The most difficult aspect of the comparison, in fact, is the inaccuracies with the measurements themselves; the extent of such inaccuracies can easily be gouged by the deviations from symmetry in certain planes, as well as comparing corresponding points where different planes intersect.

2 SCALE MODEL MEASUREMENTS

A 1/10th scale model of the fighter aircraft was constructed from polystyrene and covered with polymer sheets. The model was then copper-plated to ensure adequate conductivity. The antennas were incorporated into the model by internally guiding coaxial cable to the antenna positions and protruding the inner conductor by 30mm to form monopoles corresponding to the top-fin and bottom-fin antennas respectively.

Radiation pattern measurements in the principle planes (azimuth, side and pitch roll) were then performed on the scale model using a compact range suitable for the frequency range 2GHz-18GHz. The compact range consists of a 25 m x 10 m x 10 m anechoic chamber, calibrated feed antenna, offset parabolic reflector and positioner with three axes of freedom. The range was calibrated using a vertically polarized, standard gain horn in the frequency range 2 GHz-4 GHz. The standard gain antenna was then replaced with the scale model with the mounting bar in the same horizontal position as the standard gain antenna and the middle of the model at the same height as the standard gain antenna. The measurement system hence measured absolute gain in dB relative to an isotropic source (dBi). The only adjustment to the measured dBi values was to compute the losses in the cable leading from the calibrated connector to the antenna and to subtract these losses from the measurements in order to obtain the actual gain as measured at the antenna port.

The following movements were executed with the positioner to measure the pattern in the three principle aircraft planes (only the position and movements for the top fin antenna are given below; the bottom fin was measured using exact inverse positions and positioner movements):

- Azimuth (yaw) plane: The model was mounted horizontally and upright and simply rotated through 360°.
- Pitch plane: The model was mounted upright and horizontal, facing the receiving antenna. The model was then tilted 90° forward and 90° backwards to produce the measurement points between 0° and 180° in the plots of results. The model was then mounted facing away from the receiving antenna and again tilted 90° towards and 90° away from the receiving antenna to produce the values plotted between 180° through 360°. It is during the extremes of these tilting movements away from the receiving antenna that reflections associated with the positioner and mounting bar bending (referred to below) were most severe (corresponding to the plotted values at angles 0° and 180°).
- Roll plane: The model was mounted upright and broadside to the receiving antenna (one wing pointing towards the receiving antenna). The model was then tilted 90° towards and 90° away from the receiving antenna to produce one half of the measured points. It was then rotated by 180° and the same movements were repeated to yield the remaining values of measurements. Once again the comments above regarding errors apply with most severe cases for roll plane graph angels 90° and 270°.

It should be noted that only vertically polarized gain was measured, since this is the dominant polarization from both antennas and was also the only polarization of interest when performing link assessments. The signal source for measurements was also linked to the scale model via a cable which was always routed along the body of the scaled model to ensure that the cable enters the model at the opposite side of the model in relation to the antenna position (model mounting upright and upside down was possible using the mounting arrangement to facilitate this aim). When HF measurements on scale models were performed in the past, a stand alone source was constructed and housed inside the scale model fuselage, because at lower frequencies the aircraft electrical dimensions are small in terms of wavelengths, and the cable shield carries substantial currents which affect the measurements. At higher frequencies, however, the interaction between an antenna mounted on one side of the aircraft with the measurement cable on the opposite side is minimal. A stand alone signal source would have been a disadvantage, in the VHF/UHF case where one is interested in absolute gain values, because it would need to be custom designed with suitable calibrated characteristics.

No measurements are error-free, and measurement uncertainty is particularly difficult to ascertain when radiation patterns are measured. Using the described measurement set-up the following factors may have been the cause of some of the errors (these are more or less listed in order of their severity):

- Inaccuracies in the scale model finish and dimensions. Some of the results presented shows some signs of asymmetry which is most likely due to slight errors in curvature on either side of the antenna

- Interaction between the model and the positioner. These are most severe when the model is tilted backwards (away from the source) during roll and pitch plane measurements. This interaction manifests itself most prominently when one observes the errors in the measurements at the angles where the measured values do not coincide. (Note the 90° and 270° measurements in roll plane and the 0° and 180° points during pitch plane measurements).
- Angular errors due to a certain amount of bending in the perspex mounting bar when the model was tilted for roll and pitch plane measurements. Once again most severe for the 90° and 270° measurements in roll plane and the 0° and 180° points during pitch plane measurements.
- Rotation "wobbles" because the mount in the fuselage is not absolutely perpendicular to the fuselage horizontal datum line.
- Errors due to the fact that the protruding monopoles were not always exactly straight. This manifests itself most commonly in terms of errors in the position of the natural monopole pattern nulls.

No significant errors were caused by source amplitude instability, reflections from the chamber walls and other systematic errors associated with the range. The compact range used is professionally constructed and designed for measurements in the frequency range of interest. The calibration procedure ensures that equipment error levels are accounted for, and the quiet zone associated with the measurements is larger than the maximum movement and model dimensions during the course of the measurement manoeuvres.

3 GENERATION OF THE NUMERICAL MODELS

In this section, representations of the aircraft grid models, used for the evaluation of the top and bottom fin antennas' performance, are shown in Fig. 4 and 6. Different grid models were constructed in order to evaluate the antennas' performances at different frequencies. The numerical model uses symmetry, and therefore only half of each representative grid model is displayed. The two halves are connected at the aircraft axis of symmetry, where the segments are seen to be terminated.

The numerical models of the aircraft were constructed using the Structure Interpolation and Gridding software package, SIG [2], developed by EM-Simulations (Pty) Ltd. The SIG package generates a three-dimensional grid model from a set of user defined cross-sectional cuts at points of abrupt change along the three dimensional structure - as indicated in Fig. 3. The user-defined cross-sections shown in Fig. 3 form the basis for the grid models, shown in Figs. 4 and 5. Wings and other features attached to the main fuselage are accommodated, using the SIG package, by tagging curves which represents features in a user defined cross section and using corresponding tag numbers in later user defined cross sections. In this way, for instance, cross-section 11 in Fig. 3 consists of 3 curves with three tag numbers: The first curve represents the main fuselage, the second the top extension of the cockpit and the last curve in that cross section will just be a single point representing the start of the wing. In the next cross section (12 in Fig. 3) these three curves are re-defined with the dimensions at that cross sectional point and the curve which was tagged as the wing will in this case be a line; interpolation between the single point curve in cross section 11 and the line in cross section 12 defines the characteristic delta wing of this fighter aircraft. The ability of SIG to accommodate appendages to a fuselage in this fashion is exceedingly useful, because the gridding routine ensures that the attached features are connected at all points of the grid.

The grid models shown in Figs. 4 and 5 are generated by interpolating the cross-sectional cuts between the user defined cross-sections (in Fig. 3), at intervals which are not greater than the specified target segment lengths of the user-defined cross-sections. The segmentations produced by SIG are mainly quadrilaterals, with the side lengths approximately equal to the target segment lengths requested. Some triangular grid elements are also formed when curves expand or contract from one cross-section to the next (eg. wings regions). These triangular grid elements also have edge lengths approximately equal to the required segment length. The segment radii are calculated by the SIG package to ensure that the surface area of the segments comprising the grid is approximately twice the surface area of the structure which is modelled. Also note that SIG automatically generated segments abutting the symmetry plane which are only half the grid length to ensure grid size continuity across the symmetry plane.

The SIG program allows the user to specify a specific target segment length for every user defined cross section. This target segment length is then used until a new target length is specified in a subsequent user defined cross section. This SIG feature allowed the variable segmentation (and hence grid size) used during this study.

The use of segment lengths larger than 0.1λ significantly reduces the number of segments used in the numerical model. Generally, such a violation of the numerical modelling rules can result in an invalid numerical model. In this paper, we show that the effect of under-segmentation, in regions which are sufficiently removed from the antennas, is negligible on electrically large structures. In return, the reduction in computation time is significantly large. The effect of under-segmentation can be seen in Fig. 1 and 2, where the radiation patterns of the top-fin antenna on two different 120MHz grid models is simulated according to the segmentation schemes indicated in Table 1.

Section No. (Fig. 3)	Target segment length (120MHz)	Target segment length (120MHz)	Target segment length (220MHz)	Target segment length (300MHz)	Target segment length (400MHz)
1	0.15λ	0.25λ	0.12λ	0.18λ	0.24λ
2	0.15λ	0.25λ	0.12λ	0.18λ	0.24λ
3	0.15λ	0.25λ	0.12λ	0.18λ	0.24λ
4	0.15λ	0.25λ	0.12λ	0.15λ	0.20λ
5	0.15λ	0.25λ	0.10λ	0.12λ	0.16λ
6	0.15λ	0.25λ	0.10λ	0.10λ	0.13λ
7	0.15λ	0.25λ	0.12λ	0.16λ	0.21λ
8	0.15λ	0.25λ	0.18λ	0.22λ	0.29λ
9	0.15λ	0.25λ	0.18λ	0.22λ	0.29λ
10	0.15λ	0.25λ	0.20λ	0.24λ	0.32λ
11	0.15λ	0.25λ	0.20λ	0.24λ	0.32λ
12	0.15λ	0.25λ	0.18λ	0.25λ	0.33λ
13	0.10λ	0.10λ	0.16λ	0.22λ	0.29λ
14	0.10λ	0.10λ	0.10λ	0.13λ	0.17λ
15	0.10λ	0.10λ	0.10λ	0.10λ	0.13λ
16	0.10λ	0.10λ	0.10λ	0.15λ	0.2λ
17	0.10λ	0.10λ	0.10λ	0.15λ	0.2λ
Total No. of segment	1936	1092	4502	4982	4982

Table 1: The segmentation schemes used to generate the grid model of the aircraft at 120MHz, 220MHz, 300MHz and 400MHz.

The segmentation schemes used to generate the numerical models of the aircraft at 220MHz, 300MHz, and 400MHz, and for which theoretical results are presented in this paper, are indicated in Table 1. The total number of segments used to numerically model the aircraft in its entirety (as indicated in Table 1) are much reduced compared to that which would be required if target segments length of 0.1λ were used. Specifying a target segment length of 0.1λ would result in approximately 11400 segments for the 220MHz grid model, 20000 segments for the 300MHz grid model and 35300 segments for the 400MHz grid model.

4 PREDICTED AND MEASURED RESULTS

Appreciating the electrical size and geometrical complexity of the aircraft model, the numerically predicted radiation patterns are compared with the measured radiation patterns in Fig. 6 to Fig. 23. A close examination of the measured results reveal that while the aircraft is symmetrical, the measured patterns shows some asymmetry. In addition, at angles where two measurements were taken, repeatability errors are noted; the discussion in Section 2 gave the reasons for these asymmetry and repeatability errors. Mostly these repeatability errors are noted at points where the model was tilted backwards and the positioner interaction as well as some bending of the perspex mount caused measurement errors. Although comparison of patterns in terms of normalized values, as presented in [3, 4 and 5], are based on pattern integration on a complete volumetric data set, including both polarizations for both measured and computed patterns, the comparison between measured and theoretical results in this paper is shown in terms of absolute gains which are associated with the dominant polarization. The predicted results obtained for the lower frequencies numerical models exhibit better qualitative agreement with measured results because:

- electrically smaller size of the overall problem tends to result in simpler pattern shapes with fewer main lobes and nulls.
- they differ in their segmentation schemes (as shown in Table 1) and generally have segmentation closer to that which is required by the NEC2 modelling guide-lines [1].
- they are generally speaking less prone to numerical errors due to the smaller problem size.

The 400 MHz cases (Figs. 18 to 23) shows some cases where agreement between measurements and NEC2 results are poor, mainly due to extreme under-segmentation (0.33λ for some portions) and probably represents the limit to which this technique can be stretched. For the purpose of statistical link analysis these results were still useful, but they may be unsuitable for some more demanding evaluations.

5 CONCLUSION

The main conclusions and recommendations of this study are listed below:

- Under-segmentation of the aircraft geometry in areas removed from the antennas made the evaluation of antennas at UHF frequencies possible; without this technique most available computer resources will be inadequate for such an evaluation.
- Limited measurements (with some significant errors in some cases) proved useful in qualitatively assessing the merit of the computed results.
- Measured results can be considerably improved by changing the mounting method on scale models such that only azimuth rotation is required. This can be achieved by providing side mounts as well as front and back mounts for pitch and roll plane measurements respectively. This technique was used during subsequent studies with different aircraft and eliminated the problem of repeatable results for the same measurements points (at 0° and 360°, for instance).
- The SIG program [2] proved to be very useful for automatic grid generation of the aircraft. Particularly due to the ability to vary grid size, handle symmetry and generate grid models for different frequencies.

REFERENCES

[1] Burke, G.J. and Poggio, A.J. (1981) *"Numerical Electromagnetics Code (NEC) - Method of Moments"*, Naval Oceans Systems Centre, San Diego, C.A., 92152. Technical Document 116, Vol. 1.

[2] Structure Interpolation and Gridding (SIG) software package developed by EM-Simulations (Pty) Ltd, P O Box 1380, Pinegowrie, 2123, South Africa.

[3] Kubina, S.J. (1983) *"Numerical Modelling Methods for Predicting Antenna Performance on Aircraft"*, AGARD Lecture Series No. 131, Sept. 1983, pp 9-1 to 9-38.

[4] Peng, J., Balanis, C.A. and Britcher, C.R. (1993) *"Improvement of the NEC Code's Upper Limit and Pattern Prediction of a Helicopter Structure"*, IEEE Antennas and Propagation Society International Symposium, University of Michgan, Ann Arbor, Michigan, USA.,June 28 - July 2, 1993, Vol. 1., pp 56-59.

[5] Peng, J., Choi, J, and Balanis, C.A. (1991) *"Progress: Development of an interactive graphics program for EM codes"* 7th Annual Review of Progress in Applied Computational Electromagnetics at Naval Postgraduate School Monterey, CA., March 1991, pp 10-19.

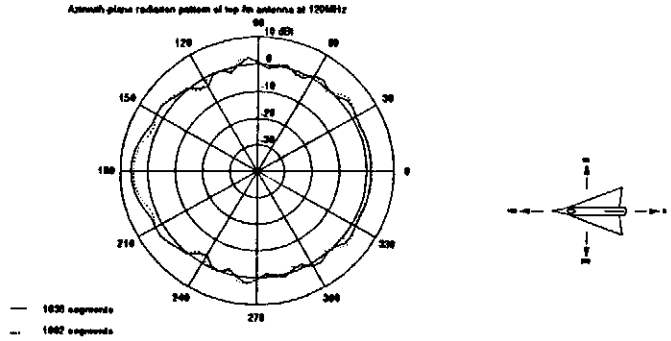

Figure 1: Theoretical azimuth-plane radiation patterns of the Top-Fin antenna at 120MHz as obtained by NEC2 for two different grid models of the fighter aircraft. Both numerical models use 0.10λ segment lengths in the vicinity of the Top-Fin antenna. In the regions which are sufficiently removed from the Top-Fin antenna, the one model uses 0.15λ segment lengths while the other model uses 0.25λ segment lengths.

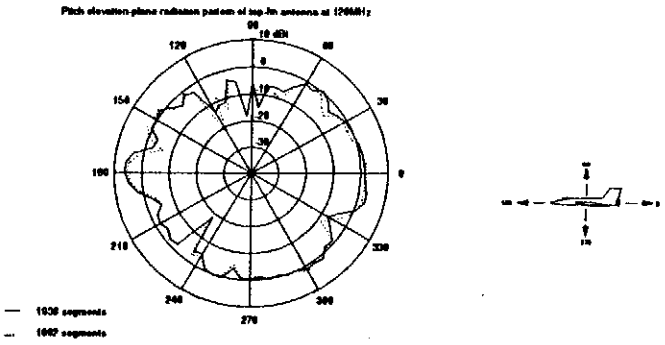

Figure 2: Theoretical pitch elevation-plane radiation patterns of the Top-Fin antenna at 120MHz as obtained by NEC2 for two different grid models of the fighter aircraft. Both numerical models use 0.10λ segment lengths in the vicinity of the Top-Fin antenna. In the regions which are sufficiently removed from the Top-Fin antenna, the one model uses 0.15λ segment lengths while the other model uses 0.25λ segment lengths.

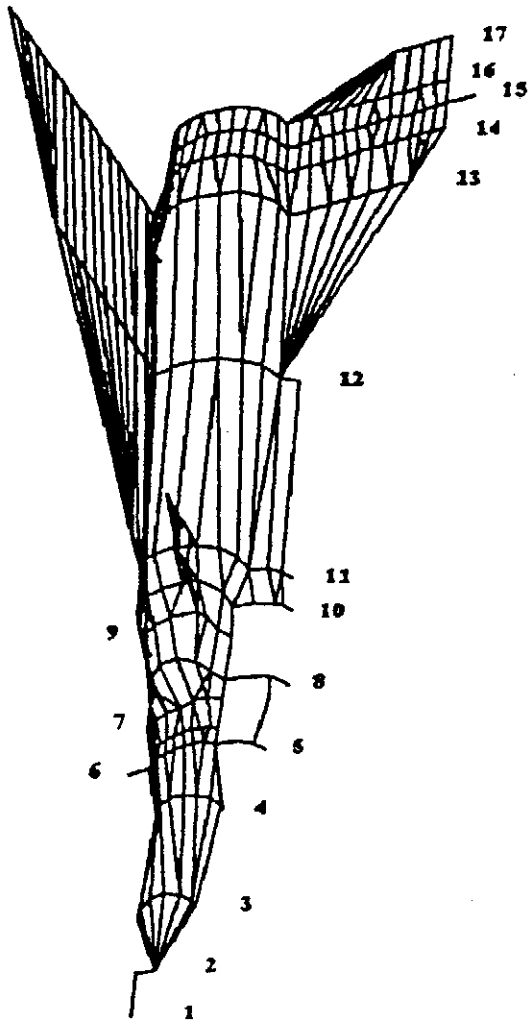

Figure 3: The user defined cross-sections used to generate the grid model of the fighter aircraft (The longitudinal lines shown in this figure are just for ease of visualizing the structure and to give an indication of the linear interpolation between the cross sections).

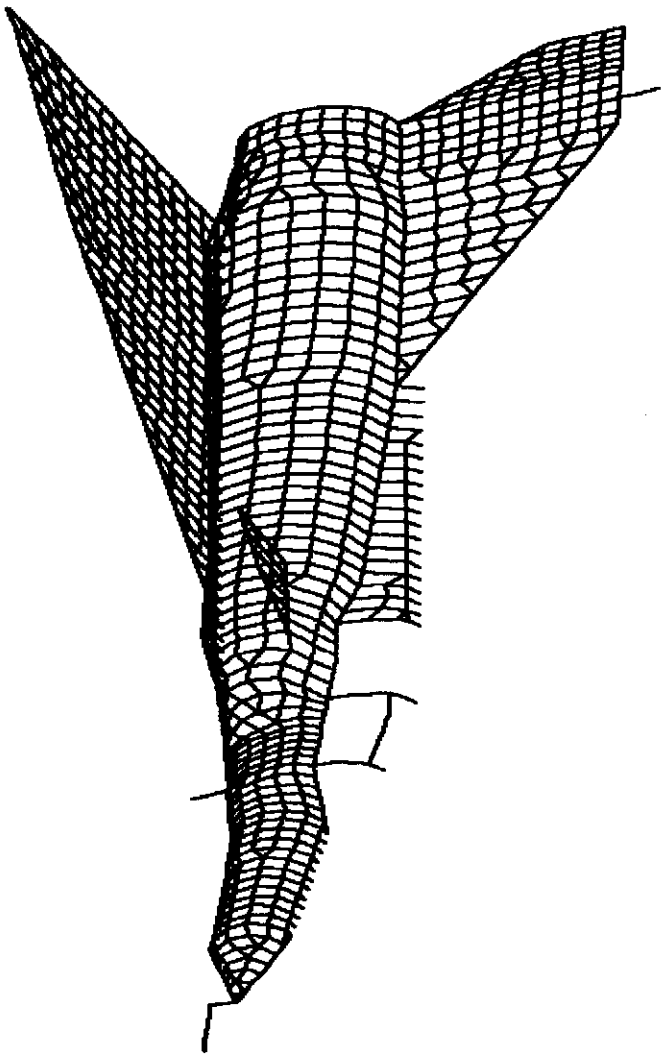

Figure 4: The grid model of the fighter aircraft at 220MHz. Since symmetry is used for simulations, only half of the grid model is displayed. The two halves are connected at the aircraft axis of symmetry where segments are seemed to be terminated. This numerical model comprises of 4502 segments with the shortest segment lengths being 0.10λ (in the vicinity of the antennas) and the longest segment lengths being 0.20λ (in a region removed from the antennas).

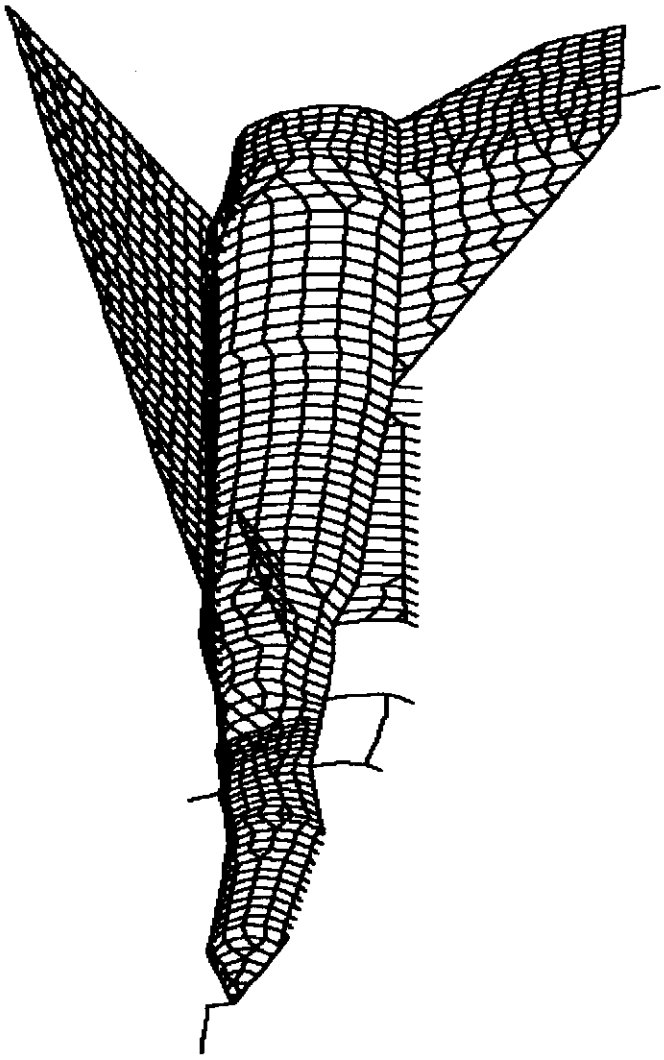

Figure 5: The grid model of the fighter aircraft at 300MHz. Since symmetry is used for simulations, only half of the grid model is displayed. The two halves are connected at the aircraft axis of symmetry where segments are seemed to be terminated. This numerical model comprises of 4982 segments with the shortest segment lengths being 0.10λ (in the vicinity of the antennas) and the longest segment lengths being 0.25λ (in a region removed from the antennas).

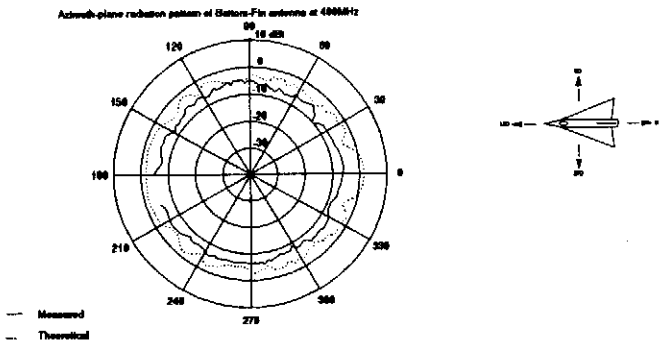

Figure 18: Measured and theoretical azimuth radiation patterns of the Bottom-Fin antenna at 400MHz. The numerical model comprises of 4982 segments with the shortest and longest segment lengths being 0.13λ and 0.33λ respectively.

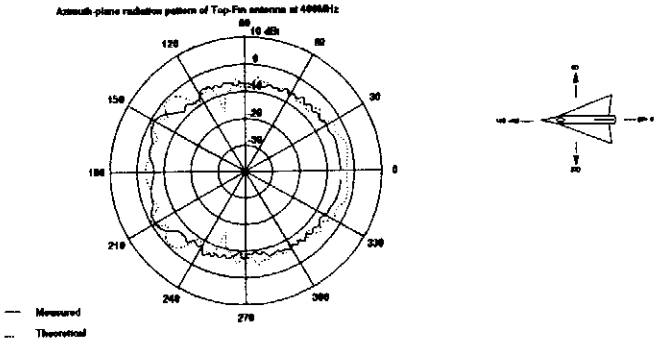

Figure 21: Measured and theoretical azimuth radiation patterns of the Top-Fin antenna at 400MHz. The numerical model comprises of 4982 segments with the shortest and longest segment lengths being 0.13λ and 0.33λ respectively.

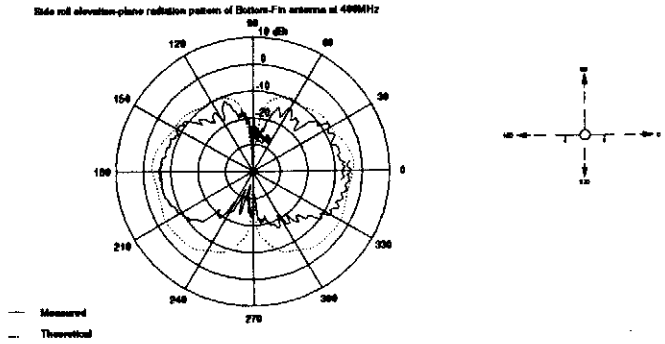

Figure 19: Measured and theoretical side roll elevation-plane radiation patterns of the Bottom-Fin antenna at 400MHz. The numerical model comprises of 4982 segments with the shortest and longest segment lengths being 0.13λ and 0.33λ respectively.

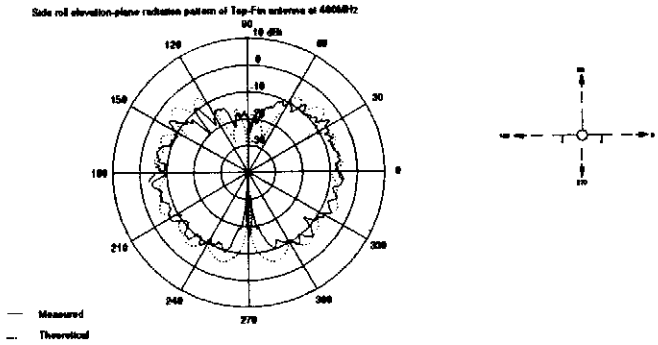

Figure 22: Measured and theoretical side roll elevation-plane radiation patterns of the Top-Fin antenna at 400MHz. The numerical model comprises of 4982 segments with the shortest and longest segment lengths being 0.13λ and 0.33λ respectively.

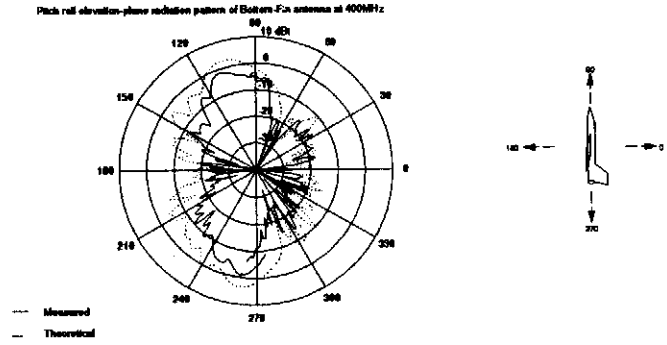

Figure 20: Measured and theoretical pitch roll elevation-plane radiation patterns of the Bottom-Fin antenna at 400MHz. The numerical model comprises of 4982 segments with the shortest and longest segment lengths being 0.13λ and 0.33λ respectively.

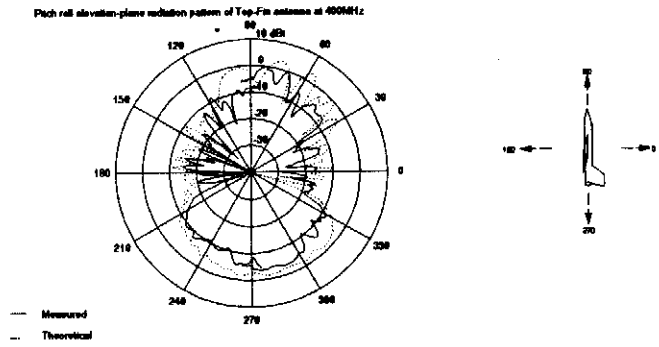

Figure 23: Measured and theoretical pitch roll elevation-plane radiation patterns of the Top-Fin antenna at 400MHz. The numerical model comprises of 4982 segments with the shortest and longest segment lengths being 0.13λ and 0.33λ respectively.